3D FEM SYSTEM FOR ANALYSIS OF INDUSTRIAL METAL FORMING PROCESSES[①]

Zuo Xu, Wei Yuanping, Chen Jun, Zeng Lingshou and Ruan Xueyu
National Die & Mold CAD Engineering Research Center,
Shanghai Jiao Tong University, Shanghai 200030, P. R. China

ABSTRACT The distinguishing techniques of 3D FEM simulation of multi-stage forming processes were presented. A CAD integrated 3D FEM simulation system, the Forming 3, has been developed to simulate the industrial multi-stage metal forming processes. Three complicated example solutions were performed using solid modeling of the forming tools. The simulation results showed good agreement with the practical results or the experimental results.

Key words bulk forming rigid-viscoplastic finite element method remeshing

1 INTRODUCTION

Due to the lack of systematic analysis tools, metal forming design is highly based on empirical idea, lots of time consuming and expensive trials are needed to complete the die and technology sequence design. In the early 1970's, Lee, Kobayashi and Zienkiewicz developed the rigid-viscoplastic flow formulation for the FEM analysis of metal forming. Because the rigid-visco plastic FEM can simulate any complicated bulk forming processes and can get detailed and comprehensive results, the method has been widely accepted as the most powerful analytical tool for the bulk forming processes. Before 1990, the researches and applications of bulk forming FEM simulation were mainly focused on 2D problems[1-2], from the end of the 80's, more and more 3D bulk forming process simulation examples were reported because of the rapid improvement of computing hardware and the Computer Aided Geometry Design (CAGD) technique. However, many researches were scholastic, they can only solve simple or simplified 3D metal forming processes[3-8], because several bottlenecks, such as the automatic generation of hexahedral mesh and the integration with CAD system, are still existing in bulk forming 3D FEM simulation.

In this paper, a CAD system integrated 3D FEM simulation system, the Forming 3, is developed to simulate complicated industrial multi-stage bulk forming processes. The paper will describe how to resolve the technical difficulties of bulk forming process in 3D FEM simulation, at last, three example solutions will be provided to demonstrate the capabilities of the Forming 3.

2 BASIC FORMULATION

The rigid-viscoplastic FEM simulation of metal forming processes is based on the Levy and Von Mises plasticity theory. To minimize the plastic work and satisfy the incompressibility condition, the bulk forming problem is expressed by a variational function:

$$\delta\pi = \int_v \bar{\sigma}\delta\dot{\bar{\varepsilon}}\,dv + \alpha\int_v \dot{\varepsilon}_{kk}\delta\dot{\varepsilon}_{mm}\,dv - \int_s F_i\delta V_j\,ds = 0 \qquad (1)$$

where α is the penalty factor.

By discreting the workpiece into many elements, Eqn. (1) is converted into the matrix formulation:

① Project 955111004 supported by the Development Foundation of Shanghai Science and Technology
Received Jul. 7, 1998; accepted Sep. 5, 1998

$$\partial \pi = \sum \frac{\partial \pi^{(m)}}{\partial \boldsymbol{u}_i} \delta u_i = 0 \qquad (2)$$

where for m element:

$$\pi^{(m)} = \sqrt{\frac{2}{3}} \iiint_{v(m)} \bar{\sigma} \cdot \sqrt{\{u\}^{\mathrm{T}}[K]\{u\}}\, \mathrm{d}v + \frac{\alpha}{2} \iiint_{v(m)} (\{\varepsilon\}^{\mathrm{T}} \cdot \{C\})^2 \mathrm{d}v - \int_{S_F(m)} \{v\}^{\mathrm{T}}\{F\}\, \mathrm{d}s \qquad (3)$$

then the matrix formulation is converted into non-linear equations which are solved by using Newton-Raphson method.

3 KEY TECHNIQUES IN 3D FEM SIMULATION OF BULK FORMING

3.1 Hexahedral mesh generation and remeshing

In the FEM simulation of bulk forming processes, large distortion of elements often occurs. Some element may even degenerate, these distorted elements may lead to an unreliable solution or terminate the simulation because of negative Jacobian determinant of elements. So, remeshing operations must be performed when severe element distortion occurs.

Usually, two kinds of element are used in 3D FEM simulation of bulk forming: 8-noded hexahedral element (referred as HEX) and 4 or 10-noded tetrahedral element (referred as TET). The simulation of the Baden-baden benchmark indicated only HEX FE models can get more accurate results[9]. However, automatic generation of hexahedral mesh for any complicated objects is a big technical difficulty in the field of CAD/CAE, also, the problem is a main bottleneck in 3D FEM simulation of bulk forming. So, many commercial FEM softwares, such as FORGE 3 and DEFORM 3D, have to employ interim method using tetrahedral element.

In this paper, two hexahedral mesh generation methods are proposed, the first one is the mapped meshing technique that divides the workpiece into simple blocks, then hexahedral meshes are mapped through these blocks by using shape function. The method is not automatic and can only be applied in relatively simple shape (such as billet).

The main algorithm of the second method is, firstly, automatically generate ten-noded curve edge tetrahedral mesh in the workpiece by using octree method, then, split each ten-noded curve edge tetrahedral element into four hexahedral elements (Fig.1) to get the fully hexahedral mesh model, then, instead of using Laplacian smoothing method, constrained mesh optimization techniques are employed to improve the quality of hexahedral mesh because the constrained mesh optimization techniques can get much better mesh qualities, specially in boundary.

The second hexahedral generation method is automatic and can be applied in any complicated shape.

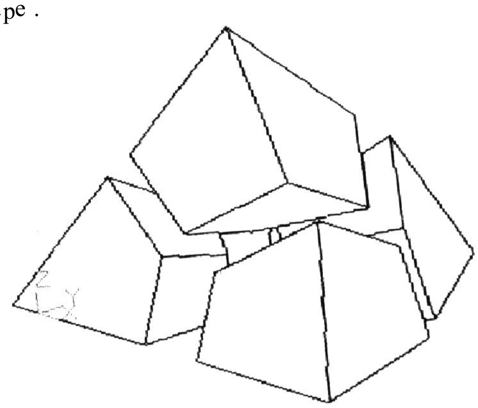

Fig.1 Split each ten-noded curve edge tetrahedral element into four hexahedral elements

To optimize the mesh quality, define the objective function F as following:

$$F = \alpha C_{ij} \cdot C_{ij} + (1 - \alpha) \sum_{m=1}^{n} (V_m - V_{m+1})^2 / V_{\max}^2 \qquad (4)$$

where V_m is the volume of element m, α is the weight factor. The C_{ij} and relative variables are defined as

$$C_{ij} = J'_{kj} \cdot J'_{kj} \qquad (5)$$

$$J'_{ij} = \frac{J_{ij}}{|\boldsymbol{J}|^{1/3}} \qquad (6)$$

where $\boldsymbol{J}$ is the Jacobian matrix of the hexahedral element.

The constrain condition is:

$$C_{dis} \leqslant 0.02 \quad (7)$$

C_{dis} is the maximum deviation of boundary nodes to boundary of the 3D object. The final problem is: minimize objective function F, and satisfy the constraint simultaneously.

The mixed discrete continuous optimization method algorithm is employed to optimize FE mesh.

The main procedure of the method is:

(1) Input or automatically produce a feasible initial vector X_0.

(2) Adopt the relative mixed subgradient (RMS) of objective function as the search direction to process discrete golden search, then, get a new vector that decreases objective function value and satisfies constraints.

The relative mixed subgradient (RMS) search direction is defined as following:

(a) The subgradient ∇f is defined as

$$\nabla f = \left[\frac{\Delta f}{\Delta x_1}, \frac{\Delta f}{\Delta x_2}, \cdots, \frac{\Delta f}{\Delta x_p}, \frac{\Delta f}{\Delta x_{p+1}}, \frac{\Delta f}{\Delta x_n} \right]^T \quad (8)$$

where $\frac{\Delta f}{\Delta x_i} = \frac{f[X + \Delta_i^+ e_i] - f[X]}{\Delta_i^+}$,

$i = 1, 2, \cdots, p$;

$\frac{\Delta f}{\Delta x_i} = \frac{f[X + \varepsilon_i e_i] - f[X]}{\varepsilon_i^+}$,

$i = p+1, p+2, \cdots, n$;

and e_i is the i th normal vector; Δ_i^+ is the i th positive increment of discrete variable; ε_i is the i th increment of continuous variable; p is the total number of discrete variables; n is the total number of all variables.

Define:

$$D = \max\left\{ \left| \frac{\Delta f}{\Delta x_i} \right| ; i = 1, 2, \cdots, p \right\} \quad (9)$$

(b) So, get the relative mixed subgradient (RMS) search direction M:

$$M = \left\{ m_i = \frac{\Delta f}{\Delta x_i} / D ; i = 1, 2, \cdots, n \right\} \quad (10)$$

(3) Take turns to repeat (2) in discrete variable field and continuous field to get a local optimum vector X_t.

(4) Search the possible better vector in neighboring field $UN(x)$, then, get the final optimum vector X^*.

The neighboring field $UN(X)$ of X is defined as:

$$UN(X) = \left\{ X \middle| \begin{array}{l} x_i + \Delta_i^- \leqslant x_i \leqslant x_i + + \Delta_i^+ ; \\ i, 2, \cdots, p \\ x_i - \varepsilon_i \leqslant x_i \leqslant x_i + \varepsilon_i ; \\ i = p+1, p+2, \cdots, n \end{array} \right\} \quad (11)$$

where Δ_i^- is the ith negative increment of discrete variable.

After the new mesh generated and optimized, the nodal values on the old mesh are transferred to the new mesh, to improve the transference precision, the hybrid transference scheme[10] is employed, that is, employ volume weight averaging scheme for internal nodes and employ least square fit scheme for boundary nodes.

3.2 Integration with CAD system

3.2.1 Description of the forming tools

In 3D FEM simulation of bulk forming, the methods of forming die description and contact algorithms are tightly associated with the CAD techniques. For a long time, the development of the FEM simulation system of metal forming is unattached with CAD system. On the other hand, the data transfer error of forming die CAD models will be avoided and the efficiency of the contact algorithm will be improved if the FEM simulation system is integrated with CAD systems.

In this paper, a CAD system integrated 3D FEM system has been developed that tightly integrates the FEM solver with the CAD system Unigraphics, I-DEAS, CATIA and Solid Works through the Parasolid data structure, the forming die models are created by using solid modeling with a CAD system. The die models are solid and all of their surfaces are NURBS surfaces. The models include precisely comprehensive geometrical information of the die and directly employed by FEM solver without any data transforming.

3.2.2 Treatment of contact

When contact takes place, the normal direction components of the workpiece node velocity must be equal to the normal components of the die velocity on the contact point, so, the contact workpiece nodes can only move along the die surface, however, after the die moving and the workpiece mesh adaptation according to the step increment, these contact nodes may break away from the die or pierce into the die surface. So, these nodes must be regulated onto the die surface. The method is: calculate the minimum distance between the nodes and the die surface (NURBS surface), then, modify the nodal position onto the die surface along the minimum distance direction. In order to avoid excessive volume loss, the displacement of die is limited in every step. Unlike other researches[6,8], the efficiency of the contact algorithm is very high because the core algorithm is to deal with the intersection of line and NURBS surface.

4 SIMULATION RESULTS

4.1 Example 1: 3D FEM simulation of an industrial multi-stage forming process

The example 1 is the multi-stage forming process simulation of a cross-shaft, a typical part in automotive industry. The simulation conditions and die shapes are defined according to the practical cases, two stages are needed in practical forming. Fig.2 shows the calculation model of the stage 1, Fig.3 shows the effective strain distribution after stage 1 finished, Fig.4 shows the

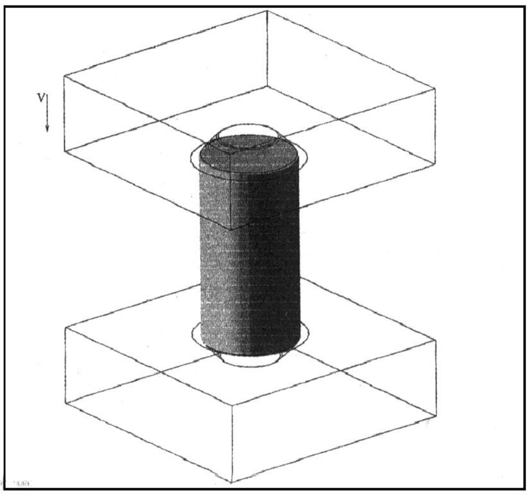

Fig.2 The calculation model of the stage 1

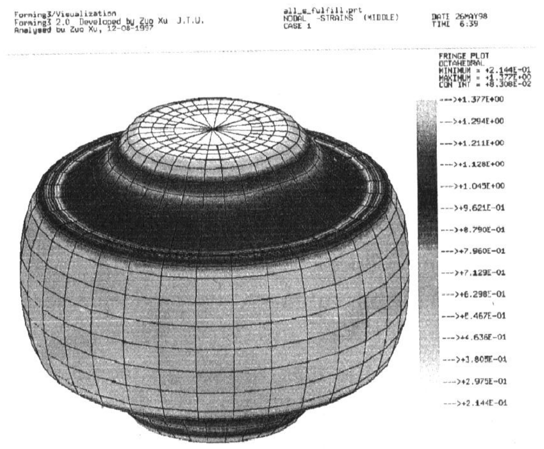

Fig.3 Effective strain distribution after stage 1 finished

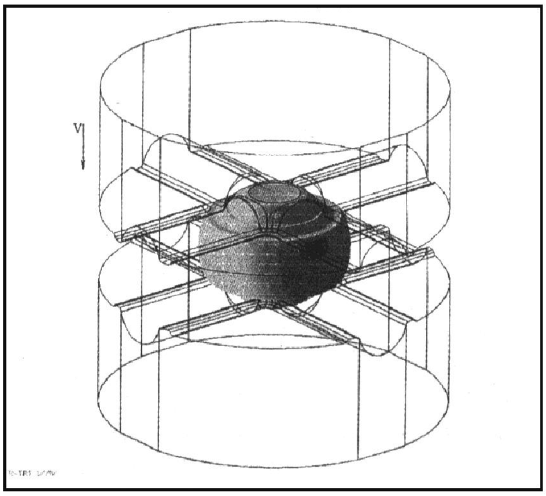

Fig.4 Calculation model of stage 2

calculation model of the stage 2, Fig.5 is the effective strain distribution after stage 2 finished. The maximum relative error rates of the flash outline between the simulation result and the practical workpiece are 8.72% (using structured mesh, that is, the mesh topology is regular) and 9.43% (using unstructured mesh, that is, the mesh topology is not regular) respectively. Five remeshing operations are needed by using structured mesh in whole simulation, on the other hand, eleven remeshing operations are needed by using unstructured mesh. The simulation results show that structured mesh can get better results than unstructured mesh.

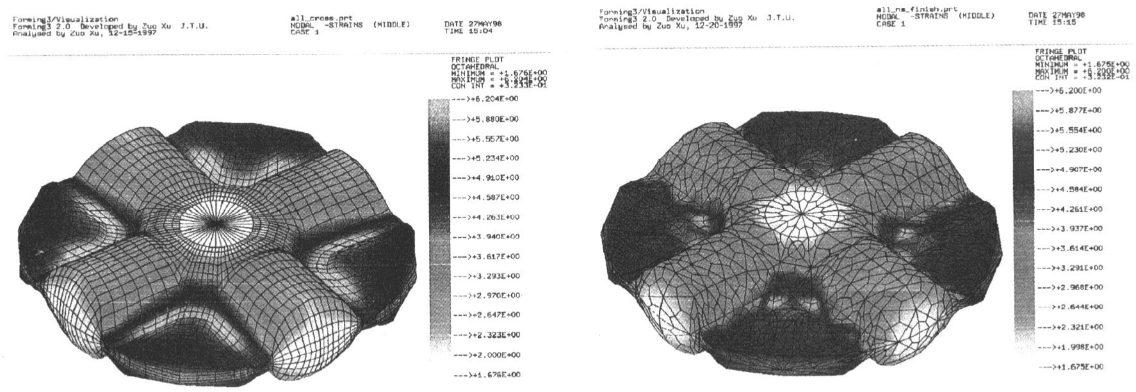

Fig.5 Effective strain distribution after stage 2 finished
(a) — Using structured mesh; (b) — Using unstructured mesh

4.2 Example 2: 3D FEM simulation of an H shaped part

The part is analyzed with structured hexahedral mesh without remeshing operation, the strain distribution of the analysis result is compared with the experimental result of photoplastic method. Fig.6 shows the effective strain distribution of the simulation result, Fig.7 shows the comparison of strain distribution between the simulation result and the experimental result.

4.3 Example 3: 3D FEM simulation of an experimental part

The part is a cross-shaft without flash bridge, the material of the part is pure Pb, three remeshing operations are performed due to the large deformation. Fig.8 shows the effective strain distribution of the simulation result, Fig.9 shows the comparison of the forming force

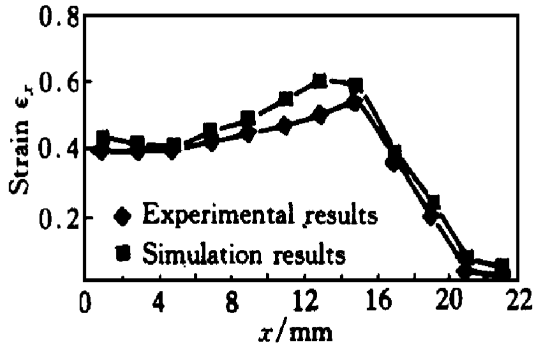

Fig.7 Comparison of the distribution of the strain when $y = 8$ mm

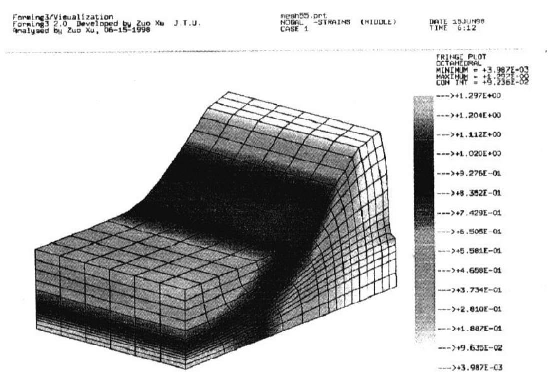

Fig.6 Effective strain distribution

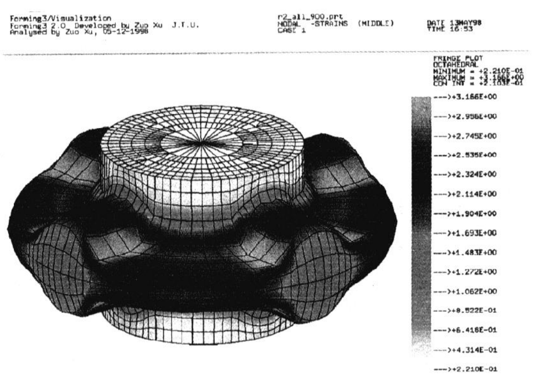

Fig.8 Effective strain distribution

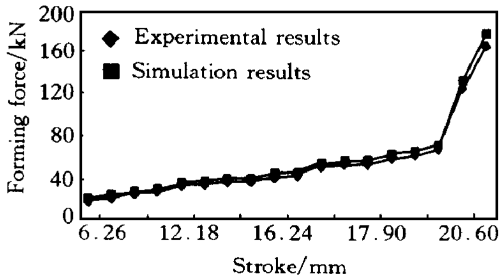

Fig.9 Comparison of the forming force between the simulation result and the experimental result.

5 CONCLUSION

The paper proposes distinguishing techniques of the 3D FEM simulation for industrial multi-stage forming processes in detail. A CAD integrated system has been developed to simulate the industrial multi-stage bulk forming processes. The simulation results show good agreement with the practical results or the experimental results. The system will show valuable help for die and process design in metal forming.

REFERENCES

1 Wei Yuanping and Ruan Xueyu. Transactions of Nonferrous Metals Society of China, 1995, 5(3): 66.

2 Wei Yuanping and Ruan Xueyu. The Chinese Journal of Nonferrous Metals, (in Chinese), 1994, 4(4): 56.

3 Li G J and Wu W T. Advanced Plasticity Technology, 1996, 25: 479.

4 Coupez Thierry. J Mater Process Technol, 1991, 27(3): 119.

5 Chen Jun, Peng Yinghong and Zuo Xu. Transactions of Nonferrous Metals Society of China, 1997, 7(4): 47.

6 Yoon J H and Yang D Y. Int J Mech Sci, 1990, 32(4): 277.

7 Rodrigues Jorge M C, Martins Paulo A F and Marques J M Barata. J Mater Process Technol, 1994, 47(3): 111.

8 Tekkaya Ahmet Erman and Kavakli Sebahattin. Steel Research, 1995, 66(2): 377.

9 Schneiders R. Engineering with Computers, 1996, 12(2): 168.

10 Oh S I, Park J and Badawy A. Advanced Plasticity Technology, 1984, 11: 1051 - 1054.

(Edited by He Xuefeng)